Optical Band Splitting and Electronic Perturbations of the Heme Chromophore in Cytochrome *c* at Room Temperature Probed by Visible Electronic Circular Dichroism Spectroscopy

Isabelle Dragomir,* Andrew Hagarman,* Carmichael Wallace,† and Reinhard Schweitzer-Stenner*

*Department of Chemistry, Drexel University, Philadelphia, Pennsylvania; and †Department of Biochemistry and Molecular Biology, Dalhousie University, Halifax, Nova Scotia, Canada

ABSTRACT We have measured the electronic circular dichroism (ECD) of the ferri- and ferro-states of several natural cytochrome *c* derivatives (horse heart, chicken, bovine, and yeast) and the Y67F mutant of yeast in the region between 300 and 750 nm. Thus, we recorded the ECD of the *B*- and *Q*-band region as well as the charge-transfer band at ~695 nm. The *B*-band region of the ferri-state displays a nearly symmetric couplet at the B_0-position that overlaps with a couplet 790 cm^{-1} higher in energy, which we assigned to a vibronic side-band transition. For the ferro-state, the couplet is greatly reduced, but still detectable. The *B*-band region is dominated by a positive Cotton effect at energies lower than B_0 that is attributed to a magnetically allowed iron → heme charge-transfer transition as earlier observed for nitrosyl myoglobin and hemoglobin. The *Q*-band region of the ferri-state is poorly resolved, but displays a pronounced positive signal at higher wavenumbers. This must result from a magnetically allowed transition, possibly from the methionine ligand to the d_{xy}-hole of Fe^{3+}. For the ferro-state, the spectra resolve the vibronic structure of the Q_v-band. A more detailed spectral analysis reveals that the positively biased spectrum can be understood as a superposition of asymmetric couplets of split Q_0 and Q_v-states. Substantial qualitative and quantitative differences between the respective *B*-state and *Q*-state ECD spectra of yeast and horse heart cytochrome *c* can clearly be attributed to the reduced band splitting in the former, which results from a less heterogeneous internal electric field. Finally, we investigated the charge-transfer band at 695 nm in the ferri-state spectrum and found that it is composed of at least three bands, which are assignable to different taxonomic substates. The respective subbands differ somewhat with respect to their Kuhn anisotropy ratio and their intensity ratios are different for horse and yeast cytochrome *c*. Our data therefore suggests different substate populations for these proteins, which is most likely assignable to a structural heterogeneity of the distal Fe-M80 coordination of the heme chromophore.

INTRODUCTION

The heme group, an iron-porphyrin derivative, is a predominant active site of redox proteins. It is well established that its structure and function are modulated by the protein environment by means of a variety of heme-protein interactions (1,2). The respective perturbations involve direct deformations of the heme structure (2,3), as well as electronic perturbations assignable to the internal electric field produced by charged, polar, and aromatic groups in the heme cavity (4,5). The influence of the latter is sometimes modulated by a network of hydrogen-bonded water molecules (6).

In principle, the most accurate method for probing asymmetric deformations of the heme group is x-ray crystallography. Indeed, crystallographic structures of various heme proteins have been used by Shelnutt, Jentzen, and associates to identify out-of-plane deformations of the heme group, which have been found to be particularly significant in cytochrome *c* isoforms (3,7). However, as recently shown, the x-ray structure might not represent the conformational average of the heme, which fluctuates between different substates (8). In-plane deformations, though functionally relevant, are generally too small to be inferable from the x-ray structure. Resonance Raman (9–10), absorption (8,11,12), EPR (13,14), NMR (15), and photon echo spectroscopy (16) provide alternative tools to detect heme-protein interactions.

In principle, electronic circular dichroism (ECD) spectroscopy is an ideal tool to probe the symmetry lowering of a highly symmetric chromophore by its environment, but a quantitative analysis is hampered by the necessity to apply a rather complex theoretical approach (17). Consequently, the number of articles in this field is rather limited. The first optical rotary dispersion (ORD) studies on horse heart cytochrome *c* have been undertaken in the sixties. Ulmer measured the ORD spectrum in the visible and UV region (18). For the Soret band, they measured a positive Cotton effect for ferro- and a negative one for the ferri-state. Additionally, their spectra suggest a couplet for the *Q*-band region of the Q_0-band. Urry and Doty (19) investigated the changes of the *B*-band Cotton effect caused by denaturation. Myer performed a more detailed study in that he investigated the temperature-, ligand-, and pH-dependence of cytochrome *c* conformation by ORD (20). Drucker et al. (21) measured the CD spectra of cytochrome c_3 derivative in the *B*- and *Q*-band regions and found again substantial differences between the ferri- and ferro-state. In all these articles, a physical rationale for the observed spectra could not be provided and the interpretation

Submitted August 25, 2006, and accepted for publication October 18, 2006.

Address reprint requests to Reinhard Schweitzer-Stenner, Tel.: 215-895-2268, E-mail: rschweitzer-stenner@drexel.edu.

0006-3495/07/02/989/10 $2.00

doi: 10.1529/biophysj.106.095976

of the Q_v-band region generally ignored its vibronic origin. The first real theoretical approach to visible heme protein ECD spectra was undertaken by Hsu and Woody for apomyoglobin and hemoglobin (20). Basically, they described the observed Cotton effect of the Soret band in terms of a coupled oscillator model involving the $\pi \rightarrow \pi^*$ transitions of the heme and nearby aromatic side chains. In a more recent study from the same research group, Blauer et al. (22) modeled the ECD-Soret band spectra of different ligation and oxidation states of the heme undecapeptide of cytochrome *c* based on a structure obtained from molecular dynamics simulations. They found a substantial intrinsic heme contribution to the Cotton signal, which arises from symmetry-lowering deformations. Additionally, they identified contributions from coupling with $\pi \rightarrow \pi^*$ transitions of the protein backbone and even higher energy transitions, which were classically modeled by polarizabilities. Kiefl et al. (23) reported a correlation between the ruffling of the heme macrocycle in carbonmonoxy myoglobin and the rotational strength in the Soret band region.

In this study, we use ECD to compare various natural cytochrome *c* isoforms. Furthermore, we investigated the Y67F mutant of yeast cytochrome *c*. In addition to the ECD spectrum of the classical B-band region, we report the *Q*-band region, which thus far has been neglected because of its low oscillator strength. Low- temperature absorption measurements and resonance Raman excitation profiles have revealed that the *Q*-band is split at cryogenic temperatures (8,24) due to the combined contributions from electronic and vibronic perturbations of the excited state (25). Mutations can affect the degree of *Q*-band splitting and asymmetry (14,26). Room temperature absorption spectra are generally thermally broadened so that neither the splitting nor the vibronic structure of the Q_v-band can be resolved. However, in the presence of a substantial band splitting, ECD spectra might provide a much better spectral resolution if the respective *x*- and *y*-components have rotational strengths of different sign. Finally, we measured the absorption and the ECD spectrum of ferricytochrome *c* in the region at ~690 nm, which displays a weak charge-transfer band, which Eaton and Hochstrasser assigned to $A_{2u}(\text{heme}) \rightarrow A_{1g}\,(d_z^2)$ transition (14). This band has been frequently used in experiments aimed at exploring the folding and unfolding of various cytochrome isoforms owing to its disappearance in the absence of the axial methionine ligand of the heme iron (27–28). This observation is consistent with an alternative assignment to a $p(\text{S}) \rightarrow d_\pi(\text{Fe}^{3+})$ transition suggested by McKnight et al. (29).

MATERIALS AND METHODS

Materials

Cytochromes *c* from horse heart (hh), chicken heart (ch), bovine heart (bh), and *Saccharomyces cerevisiae* (yeast cytochrome *c*, yc), were purchased from Sigma-Aldrich (St. Louis, MO) and dissolved in H_2O without any further purification. The yeast mutant Y67F was obtained by an earlier described procedure (6,29). The pH of all samples was adjusted to pH 6.45–7.4 by adding the appropriate HCl aliquots. Potassium ferricyanide was obtained from Fisher Scientific (Pittsburgh, PA) and sodium dithionite was obtained from Fluka (Fluka, Sigma-Aldrich).

Methods

Spectra for the *B*-band (300–500 nm) and *Q*-band (450–700 nm) regions were taken for the samples mentioned above via absorption and ECD spectroscopy for both ferri- and ferro-states using a 0.1 mM concentration for *B*-band, and a 0.5 mM concentration for *Q*-band. The only exception was the spectrum of yc Y67F, which was taken at a concentration of 0.15 mM for both *B*- and *Q*-band. For the yc Y67F mutant, only the spectra of the ferro-state were measured. A spectrum of the charge-transfer band (640–750 nm) was also taken for hh and yc at a concentration of 5.0 mM. The ferro-states were obtained by adding small quantities of sodium dithionite to the ferri samples. Because the native state of yc is partially in the ferro-state at physiological conditions, a small amount of potassium ferricyanide was added to oxidize the sample. Apart from the *Q*-band spectrum of the yc Y67F mutant, which was taken using a 2.0-mm quartz cell, all the spectra were measured in a 1.0 mm quartz cell at the Drexel University College of Medicine by employing a JASCO J-810 spectrapolarimeter (Tokyo, Japan) purged with N_2. Fifteen accumulations were taken using a 5-nm bandwidth, a 50-nm/min scanning speed, and a 0.2-nm data pitch. Additionally, a background subtraction was carried out for all the spectra using similar parameters. Room temperature variations were controlled by a Peltier heating and cooling system.

RESULTS AND DISCUSSION

B-band region

Fig. 1 *a* shows the B-band CD spectra of ferricytochrome *c* from horse heart, bovine, chicken, and yeast. The respective absorption spectra are shown in Fig. 1 *b*. For all cytochromes we observe a slightly asymmetric, negatively biased couplet with a minimum at 24 kK and a maximum at 24.7 kK, in qualitative agreement with the horse heart spectrum reported by Myer (23). The absorption peaks can be found in the vicinity of 24.5 kK. The couplet is overlaid by another positive signal at 25.5 kK. Two further minima are observed at ~26.9 and 30 kK. While the CD couplets of horse heart, bovine, and chicken cytochrome *c* are nearly identical, the respective signal of yeast cytochrome *c* is substantially weaker.

The observed couplet unambiguously reveals a splitting of the excited *B*-state, in agreement with polarized optical absorption measurements of Eaton and Hochstrasser (14). The overlapping maximum at 24.7 kK must be assigned to a vibronic side band associated with an excited state vibrational wavenumber of ≈900 cm^{-1}. To illustrate the components of the observed CD spectrum, we carried out a simulation based on the following superposition of Gaussian profiles,

$$\Delta\varepsilon(\Omega) = \sum_{i=0,1}\left[\Delta\varepsilon_i \times \exp\left(\frac{-(\Omega - \Omega_{B_{xi}})^2}{2\sigma}\right) - \Delta\varepsilon_i \times \exp\left(\frac{-(\Omega - \Omega_{B_{yi}})^2}{2\sigma}\right)\right], \quad (1)$$

where $\Delta\varepsilon_i$ is the dichroism associated with the *x*,*y* component of the $0 \rightarrow 0$ ($i = 0$) and the $0 \rightarrow 1$ transition ($i = 1$). Ω_{Bxi} and

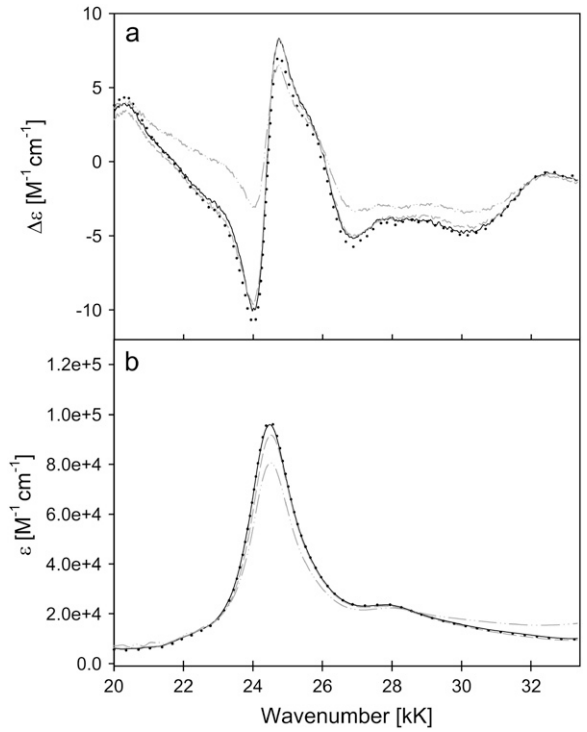

FIGURE 1 ECD (*a*) and absorption (*b*) spectra of the *B*-band region of ferri-horse heart (—), bovine (– –), chicken (· · ·), and yeast (– · · –) cytochromes *c*.

Ω_{Byi} are the respective wavenumber positions. The value σ is the Gaussian half-width, which can be inferred from the absorption spectrum. The simulation in Fig. 2 qualitatively reproduces the spectrum of, e.g., horse heart cytochrome *c*. We found that the positions of minimum and maximum do not depend on the B_{xy} splitting for splitting values below 300 cm^{-1}. A further decrease of the splitting value solely reduces the CD couplet. We assumed a splitting of 60 cm^{-1}, which corresponds to the electronic perturbation recently derived from the low temperature *Q*-band spectrum of horse heart ferrocytochrome *c* (8). The simulated spectrum was then obtained with $\Delta\varepsilon_0$ and $\Delta\varepsilon_1$ values of 120 and 30 M^{-1} cm^{-1}. The simulation demonstrates that the negative contribution of the vibronic side band overlaps with the positive part of the B_0-couplet, thus causing the observed asymmetry. We did not take into account contributions at higher wavenumbers, assignable to higher energy electronic transitions. To account for the reduced CD-couplet observed for yeast cytochrome *c*, we reduced the splitting to 30 cm^{-1}, which again corresponds to the electronic perturbation obtained from low temperature *Q*-band absorption (8). The respective simulation, which reproduces the observed decrease of the CD signal, is also shown in Fig. 2.

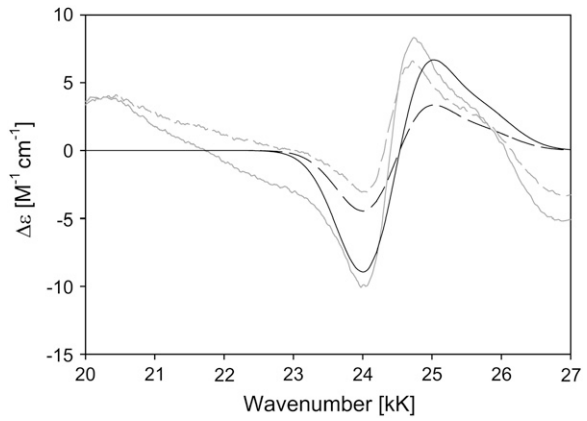

FIGURE 2 Simulation of the *B*-band ECD spectrum of horse heart (*solid line*) and yeast (*dashed line*) ferricytochrome *c* based on the superposition of two couplets described in the text. The corresponding horse heart (*shaded solid line*) and yeast (*shaded dashed line*) experimental spectra are also shown.

Fig. 3 displays the Kuhn anisotropy spectrum of horse heart ferricytochrome *c*. Apparently, the positive signal at 25.5 kK is not large enough to support an assignment to a magnetically allowed transition ($d\rightarrow\pi^*$ or $d\rightarrow d$) (30,31), thus corroborating the notion that its origin is vibronic. The vibronic side band of the Soret band itself is governed by Franck-Condon transitions of A_{1g}-modes. If one invokes a rather large frequency increase in the excited state, only the ν_7-mode (690 cm^{-1}) could be a suitable candidate (12). However, the observed frequency of ~900 cm^{-1} is very close to that of the most intense vibronic side band of the Q-band spectrum (1000 cm^{-1}), which was recently assigned to the A_{2g}-type mode ν_{22} (8). Generally, modes of this symmetry contribute only weakly to the B_v-band, but since it has the symmetry of an angular momentum, it might admix magnetic dipole strength into the corresponding B_1-state. The Kuhn anisotropy in Fig. 3 depicts another band at 20.5 kK, which reaches a maximal value of 7×10^{-4}. Addison and Stephanos identified a $d(Fe^{3+})\rightarrow$ligand CT transition at very similar wavenumbers for nitrosyl hemes (35). It is unclear whether a similar transition can occur into the *p*-orbitals of the (sixth) M80's sulfur. Alternatively, one could propose a $d_{yx}(Fe^{3+})\rightarrow\pi^*$(heme) transition, which Addison and

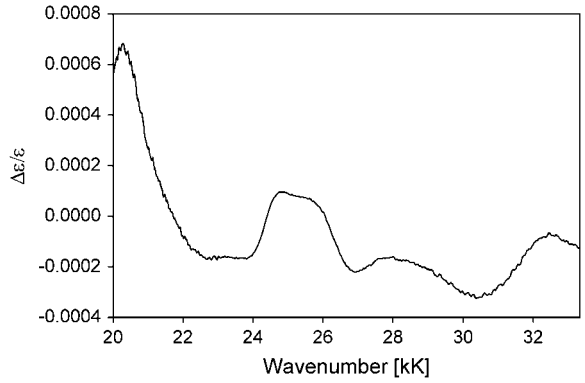

FIGURE 3 Kuhn anisotropy *B*-band spectrum of horse heart ferricytochrome *c*.

Stephanos identified in the ECD spectra of ferric Mb(II)NO at 20 kK.

The *B*-band spectra of the ferro-state of the investigated cytochromes are shown in Fig. 4. At first glance, the ECD spectra seem to be indicative of a positive Cotton effect, as reported in the literature not only for cytochrome *c*, but also for other heme proteins and for the truncated undecapeptide of horse heart cytochrome *c* (23,25). However, a closer inspection and a comparison with the absorption spectra reveal that the maximum of the positive band is substantially red-shifted ($\sim$700 cm^{-1}) with respect to the B_0-band position. At the position of the *B*-band maximum, a small but clearly discernable couplet appears, which is most pronounced for horse heart and the yeast cytochrome *c* mutant Y67F, somewhat smaller for chicken and bovine, and minimal for yeast cytochrome *c*. This couplet has not been observed in earlier measurements. We performed a simulation by invoking a superposition of a B_0 couplet with a positive Cotton-type band at lower wavenumbers. For the former, we assumed the same $\Delta\varepsilon$ values as used for the simulation of the respective ferricytochrome spectrum, but a reduced splitting, i.e., 20 cm^{-1} for horse heart and 10 cm^{-1} for yeast. The simulations in Fig. 5 reproduce the position and the magnitude of the minima and maxima for both cytochromes. The experimentally observed $\Delta\varepsilon$ values are more negative than the simulated ones on the high-energy side of the *B*-band, which clearly results from contributions of higher energy transitions not taken into consideration in our simulation. This analysis

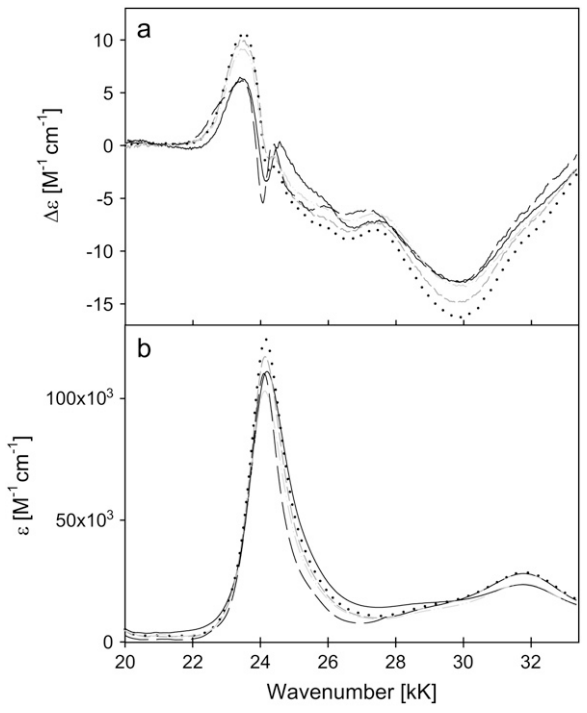

FIGURE 4 ECD (*a*) and absorption (*b*) spectra of the *B*-band region of ferro-horse heart (—), bovine (– –), chicken (· · ·), and yeast (– · · –) and Y67F mutant (— —) cytochromes *c*.

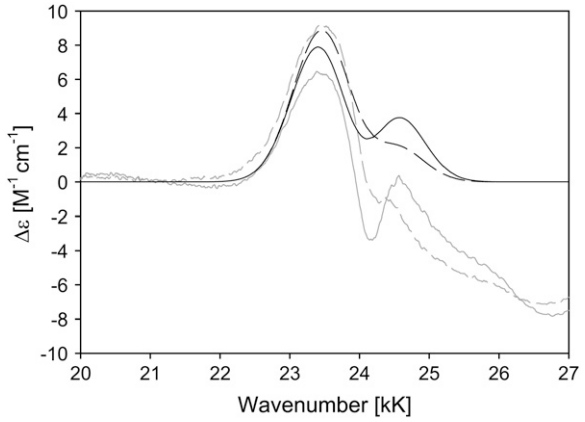

FIGURE 5 Simulation of the *B*-band ECD spectrum of horse heart (*solid line*) and yeast (*dashed line*) ferrocytochrome *c* based on the superposition of a positive Cotton band and a B_0 couplet as described in the text. The corresponding horse heart (*shaded solid line*) and yeast (*shaded dashed line*) experimental spectra are also shown.

suggests that the small couplet reflects a splitting of the *B*-state which is largest for horse heart and yeast Y67F and smallest for yeast cytochrome *c*. The values for bovine and chicken cytochrome *c* are intermediate. This resembles, though on a lower scale, the behavior of the *Q*-band splitting (14,29), as outlined in more detail below. Thus, we demonstrate that ECD spectroscopy can be used to probe even small splittings of the *B*-band, which would remain undetected in the absorption spectrum even at cryogenic temperatures.

The question arises about the origin of the positive Cotton band. The only possible explanation is that it results from a charge-transfer transition. Interestingly, Addison and Stephanos found something similar for ferrous low spin Mb(II)NO by means of optical absorption and ECD measurements, i.e., band red-shifted by $\sim$800 cm^{-1} from the B_0 band position (35). The authors assigned it to a metal $(d_\pi) \rightarrow$ porphyrin (π^*) charge-transfer transition. It is essentially electronically forbidden, but a small amount of dipole-strength can be assumed to be admixed, owing to the deviation of the symmetry from ideal D_{4h}. This explains why the band is only detectable in the ECD spectrum. The Kuhn anisotropy spectrum in Fig. 6 indicates a *g*-value of 3×10^{-4}, which is higher than the *g*-values of the *B*-band transition but too low for a pure magnetic dipole transition (34,35).

Q-band region

Fig. 7 shows the ECD and absorption spectra of the ferri-state of the investigated cytochrome *c* molecules. The Kuhn anisotropy spectrum of horse heart cytochrome *c* is displayed in Fig. 8. It covers only the region between 17 and 22 kK, because the signal to noise is low for the remaining part of the spectral region depicted in Fig. 7. A broad positive band is observed between 18 and 19 kK, which is composed of at least two bands at 18.25 and 18.96 kK. It is likely that the former is assignable to the $0 \rightarrow 0$ transition into the

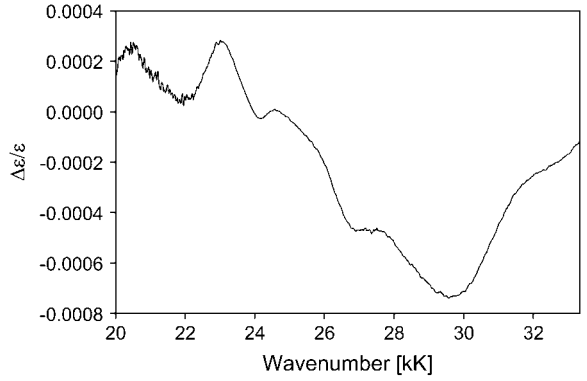

FIGURE 6 Kuhn anisotropy *B*-band spectrum of horse heart ferrocytochrome *c*.

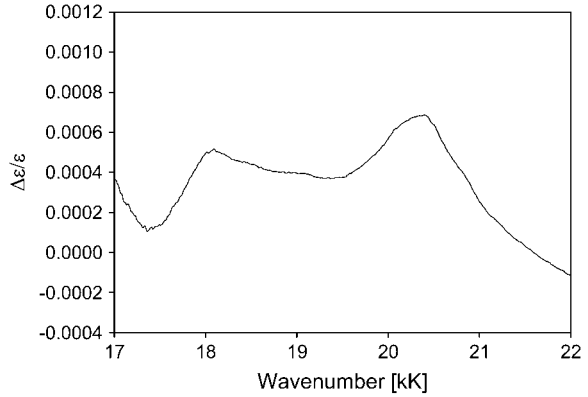

FIGURE 8 Kuhn anisotropy *Q*-band spectrum of horse heart ferricytochrome *c*.

Q-states, whereas the latter reflects some vibronic contribution. The large bandwidth associated with the individual transitions exclude the identification of individual vibronic transitions. Interestingly, the ECD displays an additional, very pronounced band at 20.34 kK, which displays a moderate anisotropy. Some somewhat smaller bands appear at 15.7 and 16.6 kK, which have an even higher anisotropy. None of these bands are assignable to classical heme→iron or iron→heme charge-transfer transitions. The two low-wavenumber bands exhibit a high Kuhn anisotropy of $\sim 10^{-3}$, which is indicative of a magnetically allowed transition (Fig. 8). A comparison with the work of Addison and Stephanos (35) on nitrosyl compounds of myoglobin and hemoglobin suggests that they might be assignable to transitions from A_{1u}, A_{2u} (15.7 and 16.6 kK), and d_{xy} orbitals (20.34 kK) into unoccupied orbitals of the sixth ligand.

Fig. 9 exhibits the ferro-state *Q*-band ECD and absorption spectra of the investigated cytochromes *c* (including Y67F). The Kuhn anisotropy spectrum of horse heart is depicted in Fig. 10 for the 17–20 kK region of the spectrum. In the Q_v-band region, the spectra nicely resolve the recently investigated vibronic structure of the Q_v-band. Normally, the

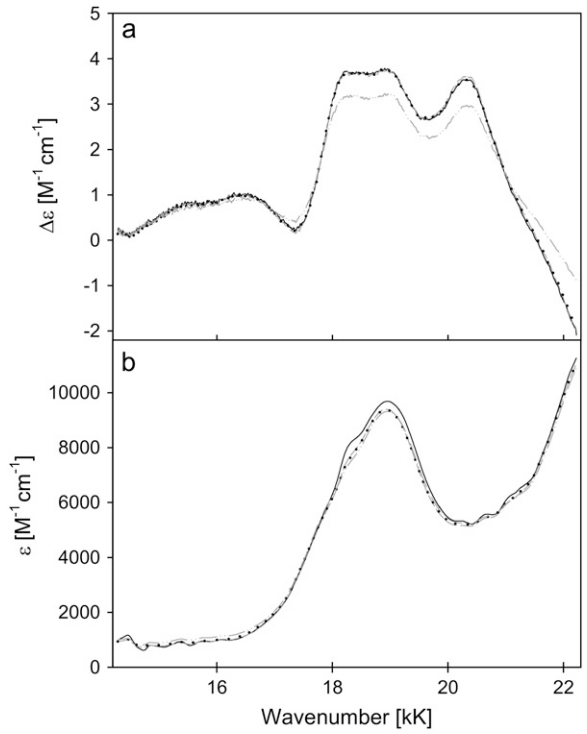

FIGURE 7 ECD (*a*) and absorption (*b*) spectra of the *Q*-band spectrum of ferri-horse heart (—), bovine (– –), chicken (· · ·), and yeast (– · · –) cytochromes *c*.

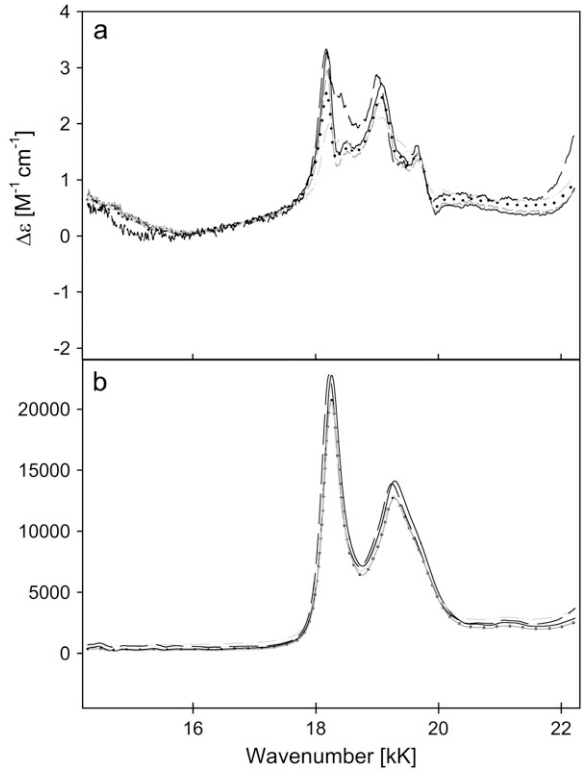

FIGURE 9 ECD (*a*) and absorption (*b*) spectra of the *Q*-band region of ferro-horse heart (—), bovine (– –), chicken (· · ·), and yeast (– · · –), and Y67F mutant (— —) cytochromes *c*.

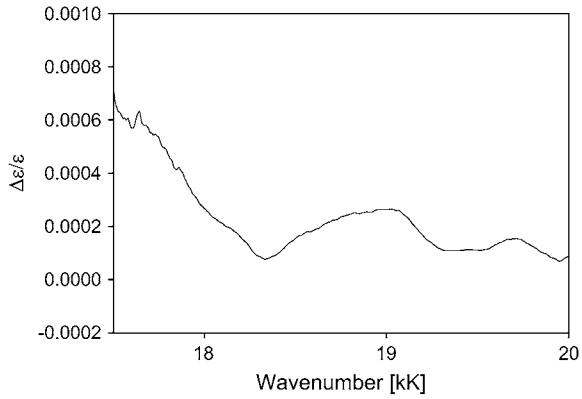

FIGURE 10 Kuhn anisotropy Q-band spectrum of horse heart ferrocytochrome c.

obtained resolution can only be achieved by low temperature absorption spectroscopy. All transitions ($0\rightarrow0$ and $0\rightarrow1$) seem to exhibit a positive Cotton effect, but a closer inspection reveals for all cytochromes c that the Q_0-band signal appears $\sim$100 cm^{-1} red-shifted from the Q_0-position, which indicates that it is assignable to the Q_x-component. The y-component has much less optical activity. It is possible that $\Delta\varepsilon_y$ is in fact negative but overlapped by positive contributions of the adjacent positive component of a vibronic transition. Three positive peaks are discernable in the Q_v-band region, which for horse heart correspond to frequency shifts of 323, 890, and 1473 cm^{-1}. From our earlier decomposition of the Q_v band (8,29), we assign the second and third value to the A_{2g}-modes ν_{22} and ν_{19}, respectively. The low frequency band is difficult to assign, but we tentatively attribute it to the previously undetected A_{2g} vibration ν_{26}, for which normal mode calculations of Ni-octaethylporphyrin predict a wavenumber of 243 cm^{-1}.

The ECD spectra reveal a hierarchy horse heart $>$ bovine $>$ chicken $\gg$ yeast with respect to the displayed rotational strength. Interestingly, the Q_0 signal of chicken cytochrome c is more reduced than those of the vibronic side bands. The effect is even more pronounced for yeast, for which the Q_0 signal is even slightly less intense than that of the vibronic side band assignable to ν_{19}.

All these observations can be explained if one assumes that all the different contributions to the Q-band are in fact asymmetric couplets with a weaker negative part overlapping with the positive part of the adjacent couplet. We illustrate this by means of a simulation based on the results of our previous analysis of the Q-band absorption (8). Adopting the approach of Schweitzer-Stenner and Bigman (28), the rotational strength of a split Q-band can be described by

$$R^{Q}_{0l,0} = R^{Q_0}_{0l,0} + \mathrm{Im}\left[\left(\sum_{\Gamma}\frac{\delta^{\Gamma}_{Q_lB_k}}{E^0_Q - E^0_B}\right)^2 \vec{\mu}_{gB_{0k}}\cdot\vec{m}_{gB_{0k}}\right], \quad (2)$$

where $R^{Q}_{0l,0}$ is the rotational strength of the transition into the unperturbed Q-states ($l = x,y$) of the 50:50 states of Gouterman's four-orbital model (32). This is supposedly very weak. The second term describes the admixture of rotational strength to the Q-states by electronic interstate coupling $\delta^{\Gamma}_{Q_lB_k}$ between Q_l and B_k ($k = x,y$) assignable to perturbation of symmetry Γ, where Γ refers to the irreducible representations A_{1g}, B_{1g}, B_{2g}, and A_{2g} of the D_{4h} point group. E^0_Q and E^0_B are the eigenenergies of the unperturbed Q_0 and B_0. $\vec{\mu}_{gB_{0k}}$ and $\vec{m}_{gB_{0k}}$ are the electronic and magnetic dipole moments for the transition from the heme ground state into the excited state B_k. Generally, the latter is zero in a nonchiral environment, but can be induced by electronic coupling between electronic transition dipole moments of the heme and the protein environment. (20,25).

The Q_v-band receives most of its intensity by vibronic mixing between Q_1 and B_0, B_2 states of several heme oscillators, predominantly of A_{2g}-symmetry,

$$R^{Q}_{0l,1}(j) = \mathrm{Im}\left[\left(\sum_{\Gamma'} c^{\Gamma'}_{Q_lB_k}(j)\right)^2\left(\frac{1}{E_{Q_l} - E_{B_k} + \Omega^{Q}_{j}} + \frac{\sqrt{2}}{E_{Q_l} - E_{B_k} + \Omega^{Q}_{j} - 2\Omega^{B}_{j}}\right)^2 \vec{\mu}_{g_0B_k}\cdot\vec{m}_{g_0B_k}\right], \quad (3)$$

where $c^{\Gamma'}_{Q_lB_K}(j)$ is the vibronic coupling operator of the j^{th} normal mode. Ω^{Q}_{j} is the frequency of the j^{th} normal mode of Q_j in the excited state, Q. For an unperturbed heme symmetry, Γ' is one of the *gerade* representations A_{1g}, of symmetry Γ, where Γ refers to the irreducible representations A_{1g}, B_{1g}, B_{2g}, and A_{2g}; in a lower symmetry, it reads as a sum of these symmetries (8). The first energy term reflects the coupling with the vibrational ground state of the electronically perturbed state B_k, the second term the interaction with the second excited vibrational state of B_k. The values E_{Q_l} and E_{B_k} are the energies of the electronically perturbed states, Q_l and B_k. For the sake of simplicity, we neglected intrastate Franck-Condon and Jahn-Teller coupling in Eq. 3.

We constructed a very heuristic model for simulating the Q-band region in Fig. 7 by using

$$\frac{|R^{Q}_{0x,i}|}{|R^{Q}_{0y,i}|} = \left(\frac{\vec{\mu}_{gQ_x}(i)}{\vec{\mu}_{gQ_y}(i)}\right)^2, \quad (4)$$

where the left-hand term is the ratio of the electronic transition dipole moments associated with the x- and y-polarized transition for the j^{th} oscillator, where $j = 0$ reflects the $0\rightarrow0$ transition. These ratios have been determined for horse heart and yeast cytochrome c by Levantino et al. (8). The square reflects the fact that the admixture of dipole strength from the B-state transitions is the same for the electronic and magnetic dipole moment. It is assumed that the natural lifetimes of the x- and y-component are identical, in agreement with resonance Raman experiments (27).

We thus simulated the Q-band ECD spectra of horse heart and yeast cytochrome c (Fig. 11) by employing the above-introduced rotational strength ratios, the band splittings, and

relative band positions reported in Levantino et al. (8) and free parameters for the prefactors of the product $\vec{\mu}_{gB_k}\vec{m}_{gB_k}$. Starting with horse heart cytochrome *c*, the latter were adjusted to approximately reproduce the experimentally observed positive peak values in the ECD spectrum. We assumed a symmetric positive couplet for each transition, which is certainly an oversimplification, but we are not aiming at a total quantitative reproduction of the spectra. Moreover, we assumed that the splitting and Stokes shift parameters observed at 20 K are approximately valid at room temperature. Despite these simplifications, the simulated ECD spectrum of horse heart ferrocytochrome *c* in Fig. 11 accounts well for the observed spectral features, thus demonstrating that the latter can indeed be rationalized as a superposition of couplets rather than of pure positive Cotton effect signals. For the simulation of yeast cytochrome *c*, we solely changed the splitting and $|R^{Q}_{0x,i}|/|R^{Q}_{0y,i}|$ values in line with the results reported by Levantino et al. (8). Thus, we observed a clear decrease of the Q_0 signal, whereas the signal of the dominant vibronic ν_{22} side band appears only slightly reduced. This is exactly what we observed experimentally, demonstrating that the differences between the ECD spectra of yeast and horse heart are predominantly due to the different electronic perturbations to which the heme groups of these two proteins are subjected. In turn, our result reveals that ECD spectroscopy is a good tool for the analysis of *Q*-band splitting even at room temperature.

The above interpretations imply that the *Q*-band splitting should reflect the experimentally observed order of the displayed rotational strength, i.e., horse heart $\gg$ bovine $>$ chicken $\gg$ yeast. This is indeed the case. Manas et al. (15) observed low temperature Q_0-band splittings of 115 cm^{-1} and 107 cm^{-1}, which are just in between the values of horse heart (116 cm^{-1}) and yeast (77 cm^{-1}).

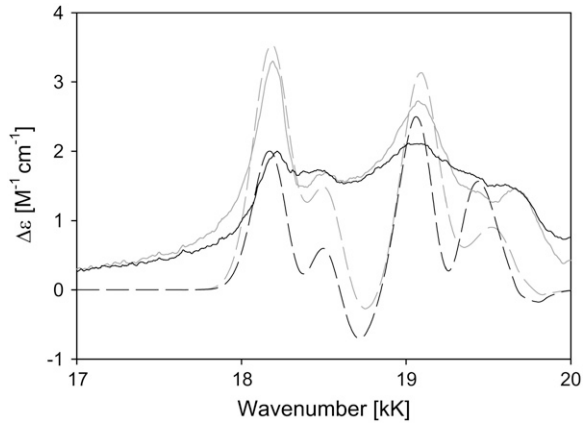

FIGURE 11 Simulation of the *Q*-band ECD spectrum of horse heart (*solid line*) and yeast (*dashed line*) ferrocytochrome *c* based on the superposition of couplets assignable to Q_0 and vibronic Q_v-side bands as described in the text. The corresponding horse heart (*shaded solid line*) and yeast (*shaded dashed line*) experimental spectra are also shown.

CT-band at 690 nm

Fig. 12 shows the ECD, the absorption spectrum, and the Kuhn anisotropy spectrum for the region between 13.3 and 15.6 kK of horse heart and yeast ferricytochrome *c*, which displays the well-known absorption band at 14.492 kK (695 nm). This band was previously assigned by Eaton and Hochstrasser to a *z*-polarized $A_{2u}(\text{heme}) \rightarrow d^2_z(Fe^{3+})$ charge-transfer transitions (14), but a comparison with the results of a more recent MCD study on low-spin ferric cytochrome P450 led McKnight et al. (33) to suggest that it results from a ligand-to-iron charge-transfer transition. Its existence depends on the axial M80 ligand of the heme iron (16–18).

To further characterize the CT band, we performed a baseline subtraction for the hh and yc ECD and absorption bands. To this end, we took the overlapping Q_0-band profile

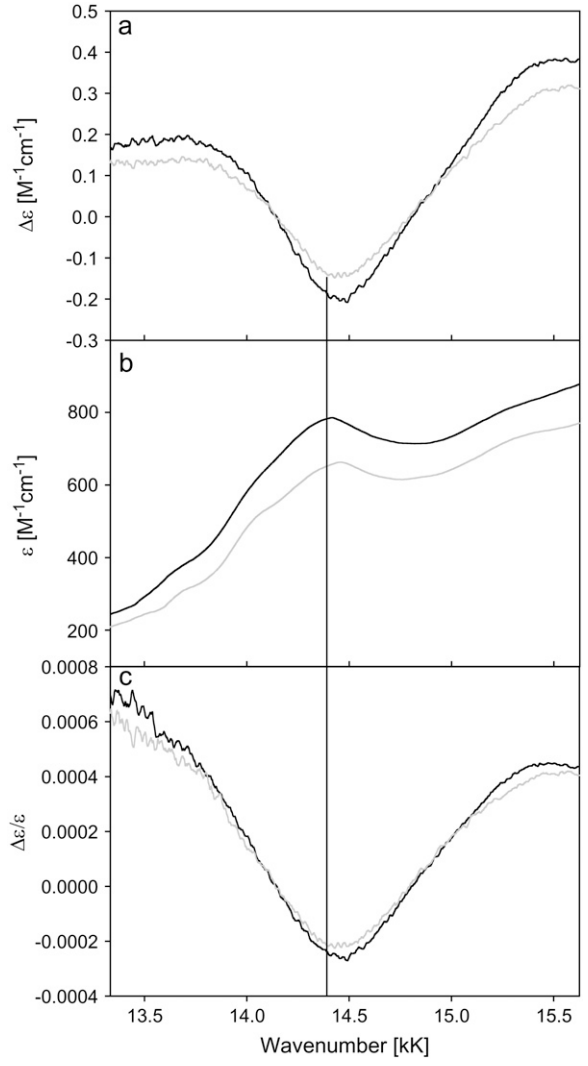

FIGURE 12 ECD (*a*), optical absorption (*b*), and Kuhn anisotropy spectra (*c*) of horse heart (—) and yeast (—) ferricytochromes *c* in the region between 13.3 and 15.6 kK.

into consideration. This was followed by a band decomposition into all Gaussian bands by our spectral analysis program MULTIFIT (33). Lorentzian contributions to the profile have been found to be negligible and were therefore omitted. For a reliable fitting, the ECD and absorption spectra were self-consistently decomposed into bands with identical parameters (i.e.: same band positions and band widths).

For horse heart cytochrome *c*, a minimal model for a simultaneous fit of the absorption and CD profile comprised three subbands at 14.02 (S2), and 14.36 (S3), and 14.70 kK (S4) (Fig. 13). The respective Gaussian half-widths are comparable. Two additional bands at 13.65 (S1) and 15.29 kK (S5) had to be added to the low energy and high-energy side, respectively, to fit the absorption spectrum. The Kuhn anisotropy spectrum in the lower panel of Fig. 12 does not exactly coincide with the position and band shape of the absorption spectrum. This indicates that the different subbands have different anisotropy values. A comparison of the maxima of the respective subbands indeed reveals slightly different *g*-values, namely -1.56×10^{-4}, -2.22×10^{-4}, and -1.18×10^{-4} for S2, S3, and S4, respectively. All these values are indicative of electronically allowed transitions (34). S1 and S5 do not show any detectable rotation strength.

A similar band-decomposition for yc was also performed using analogous parameters (Fig. 14). Thus, we obtained again

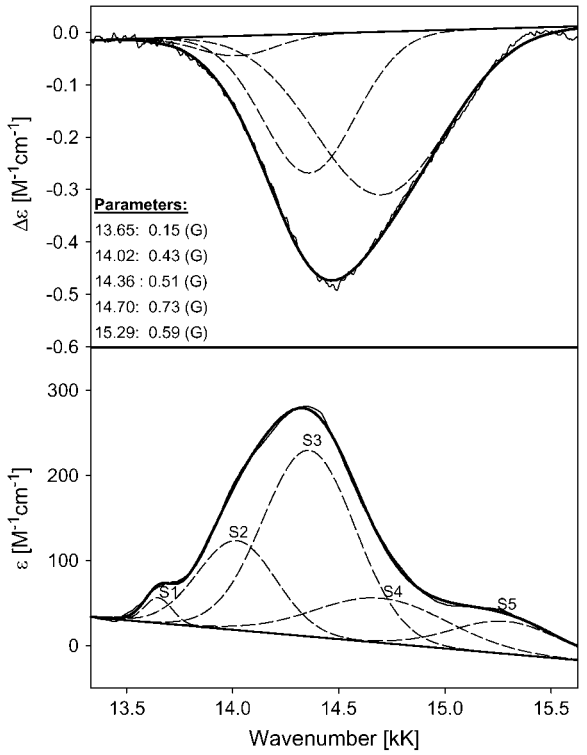

FIGURE 13 Decomposition of the charge-transfer band of horse heart cytochrome *c* at 14 kK as described in the text. The band parameters are listed on the figure.

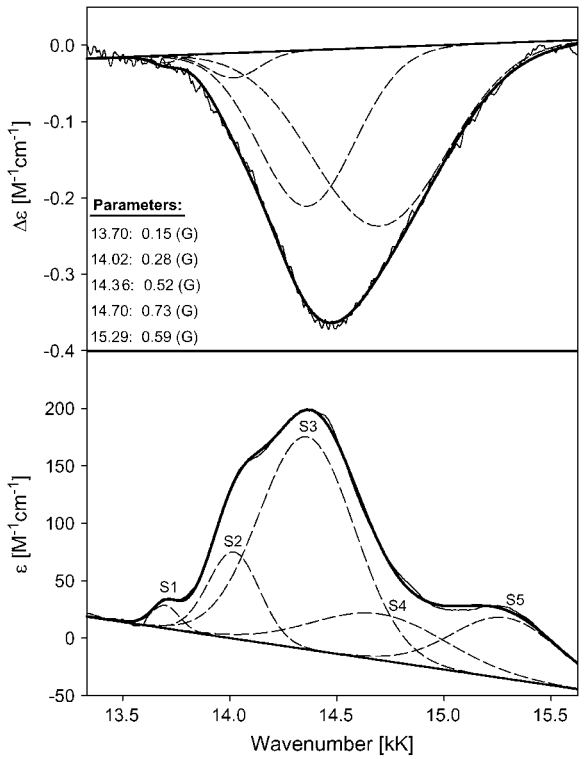

FIGURE 14 Decomposition of the charge-transfer band of yeast cytochrome *c* at 14 kK as described in the text. The band parameters are listed on the figure.

a three-band fit, with bands at 14.02 (S2), 14.36 (S3), and 14.70 kK (S4) for the absorption and CT spectra, with two additional bands at 13.70 (S1) and 15.29 kK (S5) for the absorption spectrum. With the exception of S2, which shows a narrower bandwidth (0.15 kK) for yc than for hh (0.21 kK), all subbands have the same Gaussian bandwidth and peak positions as the corresponding hh subbands. The Kuhn anisotropy values are -1.29×10^{-4} (S2), -1.93×10^{-4} (S3), and -9.34×10^{-5} (S4). The respective absorption intensity ratios $\varepsilon_{hw}/\varepsilon_{lw}$ (*hw*, high wavenumber; *lw*, low wavenumber) are 10.1 (S2/S1) and 24.9 (S3/S1), 8.5 (S4/S1), and 5.0 (S5/S1) for hh and 6.9 (S2/S1) and 31.3 (S3/S1), 9.5 (S4/S1), and 10.1 (S5/S1) for yc. These reflect a significant difference between the intensity distributions of the CT bands of hh and yc.

Eaton and Hochstrasser have attributed the 695-nm band to an $A_{2u}(\text{heme}) \rightarrow A_{1g}(d_z^2)$ transition (14). This assignment does not really explain why the band disappears when the sixth ligand is exchanged without altering the iron's spin state (30–32). This observation is, however, consistent with the proposal of McKnight et al. (33), who attributed this band to a $p(\text{S}) \rightarrow d_\pi(\text{Fe}^{3+})$ transition where S is the sulfur atom of the methionine ligand. The authors discussed four scenarios. If the d_π hole is predominantly d_{xz}, the possible transitions are $p_x \rightarrow d_{xz}$ and $p_z \rightarrow d_{xz}$ with *z* and *x* polarization, respectively. A predominant d_{xy} character of d_π brings

about the *x*- and *y*-polarized transitions $p_y \rightarrow d_{xy}$ and $p_x \rightarrow d_{xy}$. The third possibility is that d_π is mainly d_{yz}, the respective transitions are $p_y \rightarrow d_{yz}$ and $p_z \rightarrow d_{yz}$ with *z* and *y* polarization. The fourth possibility would involve a mixture of all three cases. However, the polarized absorption measurements of Eaton and Hochstrasser suggest a *z* polarization with some *x* or *y* admixture which is consistent with d_π being predominantly d_{xz} or d_{yz} (14). In the presence of d_π-splitting due to the rhombic deformations revealed by resonance Raman and absorption data (8,10,29), one expects d_{yz} to be the highest lying occupied *d*-orbital. McKnight et al. (33) arrived at the same conclusion for the CT band in the spectrum of cytochrome P-450 *Bacillus megaterium*.

This interpretation seems to suggest that the observed subbands of the CT band are assignable to different $p(S) \rightarrow d_\pi(Fe^{3+})$ transitions, but some observations are at variance with this conclusion. First of all, the MCD data reported by McKnight et al. (33) suggest a wavenumber difference of nearly 1 kK between, e.g., $p_y \rightarrow d_{yz}$ and $p_z \rightarrow d_{yz}$. The wavenumber differences between the CT-subbands are much smaller. Second, a pure electronic nature of the observed subbands could hardly explain the spectral differences between yeast and horse heart cytochrome *c*. Third, if at least some of the subbands were due to transitions of orthogonal polarization, one would expect a couplet rather than a continuously negative Cotton effect. We therefore suggest that the observed band structure reflects predominantly conformational heterogeneity, i.e., the coexistence of conformational substates, which give rise to a distribution of wavenumbers for the investigated transition. Hence, we tentatively assign the subbands S2-S4 to the same $p_y \rightarrow d_{yz}$ transition in different taxonomic substates, whereas the small but always reproducible sideband at 13.65 kK (hh) and 13.70 kK (yc) might be assignable to the $p_z \rightarrow d_{yz}$ transition. This interpretation resembles observations made for the classical band III of deoxymyoglobin and hemoglobin (34–35). The spectral differences between horse heart and yeast cytochrome *c* would thus reflect different conformational distributions, which most likely reflect different methionine orientations. The existence of conformational substates have earlier been inferred from spectral hole burning experiments and molecular dynamics calculations by Köhler et al. (4) and Laberge et al. (36). They identified two spectroscopically discernable taxonomic substates for horse heart Zn-cytochrome *c*, whereas only one of them could be identified for the respective yeast protein. It has to be emphasized that our band decomposition might be based on an oversimplified model in that we assume that each taxonomic substate is describable by a symmetric Gaussian line. In reality, a more asymmetric distribution reflecting further heterogeneity on a lower tier might be a more appropriate model (37). A final clarification of the issue, however, has to await additional experiments (e.g., investigation of the temperature and pH dependence of the CT band's substructure) which are currently underway in our laboratory.

We thank Bruce Stewart, Dalhousie University, for the expert expression and purification of the mutant cytochromes.

Financial support was provided from a grant from the National Science Foundation (grant No. MCB-0318749) to R.S.S. and from the Natural Sciences and Engineering Research Council of Canada to C.W.

REFERENCES

1. TenEyck, L. F. 1979. Hemoglobin and myoglobin. *In* The Porphyrins, Vol. III. D. Dolphin, editor. Academic Press, New York.
2. Schweitzer-Stenner, R. 1989. Allosteric linkage-induced distortions of the prosthetic group in haem proteins as derived by the theoretical interpretation of the depolarization ratio in resonance Raman scattering. *Q. Rev. Biophys.* 22:381–479.
3. Jentzen, W., J.-G. Ma, and J. A. Shelnutt. 1998. Conservation of the conformation of the porphyrin macrocycle in hemoproteins. *Biophys. J.* 74:753–763.
4. Köhler, M., J. Gafert, J. Friedrich, J. M. Vanderkooi, and M. Laberge. 1996. Stark–effect experiments in cytochrome *c*-type proteins: structural hierarchies. *Biophys. J.* 71:77–85.
5. Laberge, M. 1998. Intrinsic protein electric fields: basic non-covalent interactions and relationships to protein-induced Stark effects. *Biochim. Biophys. Acta.* 1386:305–330.
6. Blouin, C., and C. J. A. Wallace. 2001. Protein matrix and dielectric effect in cytochrome *c*. *J. Biol. Chem.* 276:28814–28818.
7. Jentzen, W., X.-Z. Song, and J. A. Shelnutt. 1997. Structural characterization of synthetic and protein-bound porphyrins in terms of the lowest-frequency normal coordinates of the macrocycle. *J. Phys. Chem. B.* 101:1684–1699.
8. Levantino, M., Q. Huang, A. Cupane, M. Laberge, A. Hagarman, and R. Schweitzer-Stenner. 2005. The importance of vibronic perturbations in ferrocytochrome *c* spectra: a reevaluation of spectral properties based on low-temperature optical absorption, resonance Raman, and molecular-dynamics simulations. *J. Chem. Phys.* 123:054508.
9. Shelnutt, J. A., D. L. Rousseau, J. K. Dethmers, and E. Margoliash. 1981. Protein influences on porphyrin structure in cytochrome *c*: evidence from Raman difference spectroscopy. *Biochemistry.* 20:64895–66497.
10. Döpner, S., P. Hildebrandt, F. I. Rosell, and A. G. Mauk. 1998. Alkaline conformational transitions of ferricytochrome *c* studied by resonance Raman spectroscopy. *J. Am. Chem. Soc.* 120:11246–11255.
11. Eaton, W., and R. M. Hochstrasser. 1968. Single-crystal spectra of ferrimyoglobin complexes in polarized light. *J. Chem. Phys.* 49:985–995.
12. Manas, E. S., J. M. Vanderkooi, and K. A. Sharp. 1999. The effect of protein environment on the low temperature electronic spectroscopy of cytochrome *c* and microperoxidase-11. *J. Phys. Chem. B.* 103:6334–6348.
13. Schejter, A., and W. A. Eaton. 1984. Charge-transfer optical spectra, electron paramagnetic resonance, and redox potentials of cytochromes. *Biochemistry.* 23:1081–1084.
14. Kerfeld, A. C., M. R. Sawaya, H. Bottin, K. T. Tran, M. Sugiura, D. Cascio, A. Desbois, T. O. Yeates, D. Kirilovsky, and A. Boussac. 2003. Structural and EPR characterization of the soluble form of cytochrome *c*-550 and of the *psbV2* gene product from the cyanobacterium *Thermosynechoccus elongates*. *Plant Cell Physiol.* 44:697–706.
15. Schejter, A., G. Taler, G. Navon, X. J. Liu, and E. Margoliash. 1996. Oxidation state-induced change of iron ligand in the phenylalanine-82 to histidine mutant of yeast iso-1-cytochrome *c*. *J. Am. Chem. Soc.* 118:477–478.
16. Cho, B. M., F. Carlsson, and R. Liminez. 2006. Photon echo spectroscopy of porphyrins and heme proteins: effects of quasidegenerate electronic structure on the peak shift decay. *J. Chem. Phys.* 124:144905.
17. Hsu, M.-C., and R. W. Woody. 1971. The origin of the heme cotton effects in myoglobin and hemoglobin. *J. Am. Chem. Soc.* 93:3515–3525.
18. Ulmer, D. D. 1965. Optical rotary dispersion of oxidized and reduced cytochrome *c*. *Biochemistry.* 4:902–907.

19. Urry, D. W., and P. Doty. 1965. On the conformation of horse heart ferri- and ferrocytochrome *c*. *J. Am. Chem. Soc.* 87:2756–2758.

20. Myer, Y. P. 1968. Conformation of cytochromes. III. Effect of urea, temperature, extrinsic ligands and pH variation on the conformation of horse heart ferricytochrome *c*. *Biochemistry.* 7:765–776.

21. Drucker, H., L. L. Campbell, and R. W. Woody. 1970. Optical rotary properties of the cytochrome *c*8 species of *Desulfovibrio*. *Biochemistry.* 9:1519–1527.

22. Blauer, G., N. Sreeama, and R. W. Woody. 1993. Optical activity of hemoproteins in the Soret region: circular dichroism of the undecapeptide of cytochrome *c* in aqueous solution. *Biochemistry.* 32:6674–6679.

23. Kiefl, C., N. Sreerama, R. Haddad, L. Sun, W. Jentzen, Y. Lu, Y. Qiu, J. A. Shelnutt, and R. W. Woody. 2002. Heme distortions in sperm-whale carbonmonoxy myoglobin: correlations between rotational strengths and heme distortions in MD-generated structures. *J. Am. Chem. Soc.* 124:3385–3394.

24. Friedman, J. M., D. L. Rousseau, and F. Adar. 1977. Excited state lifetimes in cytochromes measured from Raman scattering data: evidence for iron-porphyrin interactions. *Proc. Natl. Acad. Sci. USA.* 74:2607–2611.

25. Schweitzer-Stenner, R., and D. Bigman. 2001. Electronic and vibronic contributions to the band splitting in optical spectra of heme proteins. *J. Phys. Chem. B.* 105:7064–7073.

26. Schweitzer-Stenner, R., M. Levantino, A. Cupane, C. Wallace, M. Laberge, and Q. Huang. 2006. Functionally relevant electric-field induced perturbations of the prosthetic group of yeast ferrocytochrome *c* mutants obtained form a vibronic analysis of low-temperature absorption spectra. *J. Phys. Chem. B.* 110:12155–12161.

27. Davis, L. D., A. Schejter, and G. P. Hess. 1974. Alkaline isomerization of oxidized cytochrome *c*. *J. Biol. Chem.* 249:2624–2632.

28. Taler, G., A. Schejter, G. Navon, I. Vig, and E. Margoliash. 1995. The nature of the thermal equilibrium affecting the iron coordination of ferric cytochrome *c*. *Biochemistry.* 34:14209–14212.

29. McKnight, J., M. R. Cheesman, A. J. Thoson, J. S. Miles, and A. W. Munro. 1993. Identification of charge-transfer transitions in the optical spectrum of low-spin ferri cytochrome P-450 *Bacillus megaterium Eur. J. Biochem.* (*Tokyo*). 213:683–687.

30. Gillard, R. D. 1968. Optical rotary dispersion and circular dichroism. *In* Physical Methods in Advanced Inorganic Chemistry. H. A. O. Hills and P. Day, editors. Interscience, London.

31. Addison, A. W., and J. J. Stephanos. 1986. Nitrosyliron(III) hemoglobin: autoreduction and spectroscopy. *Biochemistry.* 25:4104–4113.

32. Gouterman, M. 1959. Study of the effects of substitution on the absorption spectra of porphyrin. *J. Chem. Phys.* 30:1139–1161.

33. Jentzen, W., E. Unger, G. Karvounis, J. A. Shelnutt, W. Dreybrodt, and R. Schweitzer-Stenner. 1996. Conformational properties of nickel(II) octaethylporphyrin in solution. 1. Resonance excitation profiles and temperature dependence of structure sensitive Raman lines. *J. Phys. Chem.* 100:14184–14191.

34. Campbell, B. F., M. R. Chance, and J. M. Friedman. 1987. Linkage of functional and structural heterogeneity in proteins: dynamic hole burning in carbonmonoxy myoglobin. *Science.* 238:373–376.

35. Gilch, H., R. Schweitzer-Stenner, W. Dreybrodt, M. Leone, A. Cupane, and L. Cordone. 1996. Conformational substates of the $Fe^{2}+$-His F8 linkage in deoxymyoglobin and hemoglobin probed in parallel by the Raman band of the Fe-His stretching vibration and the near infrared absorption band III. *Int. J. Quant. Chem.* 59:301–313.

36. Laberge, M., M. Köhler, J. M. Vanderkooi, and J. Friedrich. 1999. Sampling field heterogeneity at the heme of c-type cytochromes by spectral hole burning spectroscopy and electrostatic calculations. *Biophys. J.* 77:3293–3304.

37. Ansari, A., J. Berendzen, S. F. Bowne, H. Frauenfelder, I. E. T. Iben, T. B. Sauke, E. Shysamunder, and R. D. Young. 1985. Protein states and protein quakes. *Proc. Natl. Acad. Sci. USA.* 85:5000–5004.